コンクリート工学年次論文報告集, Vol.16, No.2, 1994

論 文

[2138] Seismic Behavior of Precast Beam-Column Joints with Eccentricity

Juan J. CASTRO[*1], Teruaki YAMAGUCHI[*2] and Hiroshi IMAI[*3]

1. INTRODUCTION

A new concept was proposed to joint precast concrete members for frame-type structures [1]. Here the precast concrete members are jointed at the end of the members through concrete cast in-situ at the beam-column joint, and the bar connections are located at the middle of precast members where the stresses due to seismic forces are small.

The frame type buildings, due to architectural characteristics, present sometimes difficult configurations, that make the axes of the beams have eccentricity with respect to the column axes. Some studies on beam-column joints with eccentricities have been carried out in the past, specially on beam-column joints with wider columns and deeper beams with one side eccentricity. Also the seismic behavior of interior beam-column joints with various geometrical configurations was studied [2]. In all cases they were carried out for monolithic reinforced concrete specimens.

The present research was carried out to investigate the influence of the eccentricity on the seismic behavior of precast concrete beam-column joints. Also the effective width of the beam-column joint that contributes to resist the shear stress, and the contribution of the lateral reinforcement of beam-column joints with supplementary cross ties were studied.

2. SPECIMEN AND EXPERIMENTAL PROGRAM

Six specimens with 2/3 scale were tested. The dimensions of the test specimens are shown in Fig. 1. Description of the specimens is given in Table 1. All the specimens were designed to fail in shear at the beam-column joint.

When the precast members were cast, corrugated metal ducts (sheaths) were placed at the position of the main bars. Once the precast columns and beams were positioned, the lower main bars of the beams were inserted into the sheaths, so that the bars passed straightly through the beam-column joints. The joint shear reinforcement and upper beam bars were also placed in this stage. Once the column main bars were inserted from the upper side, high strength mortar was grouted inside the sheath of column. Next step was to cast concrete in the upper part of the beam, slab and joint as well.

*1 Graduate School, University of Tsukuba, M.Sc., Member of JCI
*2 Technical Research Institute, Kabuki Construction Co. Ltd., Member of JCI
*3 Institute of Engineering Mechanics, University of Tsukuba, Dr. Eng., Member of JCI

Finally after the upper column was set and its bottom sealed, high strength mortar was grouted. At this step the beam lower main bars were also grouted.

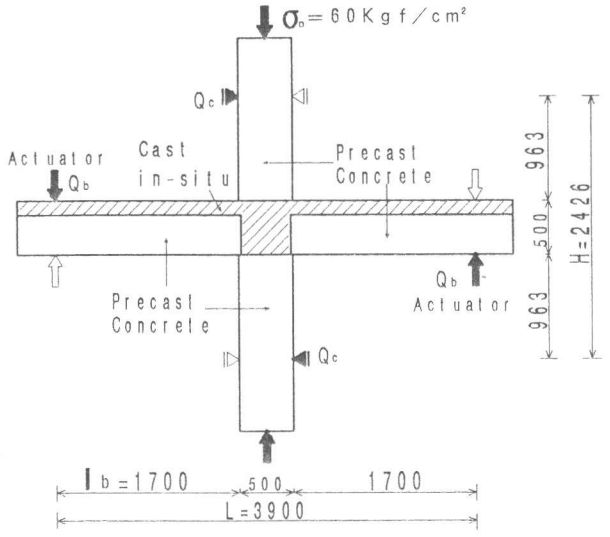

Fig. 1 Test specimen

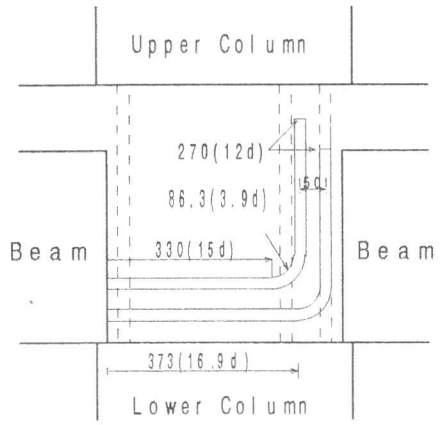

Fig. 2 Detail of bent up bars

Specimen JPC-31 without eccentricity is considered as the standard specimen. There were two groups of specimens. The first group is composed by JPC-31, JPC-32 and JPC-33. Specimens JPC-31 and JPC-32 had the beams shifted in opposite directions (opposite side eccentricity) with respect to the center of the column. These specimens have eccentricities of 4 cm and 8 cm, respectively. The beam bars were placed in two layers, and due to the opposite side eccentricity, there were only some bars passing straightly through the joint, and the rest were bent passing the center of the column, as shown in Fig. 2. The total anchor length inside the joint was 31 times the bar diameter (31d). The horizontal anchor length was 16.9 d for the first layer and 15 d for the second layer. The section of columns is shown in Fig. 3.

Table 1 Characteristics of specimens

SPECIMEN Eccentricity (cm)		JPC-31 0	JPC-32 4	JPC-33 8	JPC-34 0	JPC-35 4	JPC-36 8
B E A M	Section	34cm x 50 cm					
	Main Bars	8-D22 pt= 2.19 %					
	Stirrups	4-D13@80 pw= 1.86 %					
C O L U M N	Section B x D(cm)	58 x 50	58 x 50	58 x 50	42 x 50	50 x 50	58 x 50
	Main Bars	22-D19	20-D19	22-D19	18-D19	20-D19	22-D19
	Reinf. Ratio pt(%)	0.89	0.79	0.89	0.95	0.91	0.89
	Hoops	6-D10@100			4-D10@100	6-D10@100	
	Reinf. Ratio pw(%)	0.74			0.68	0.86	0.74
	ΣMcu / ΣMbu	1.45	1.37	1.45	1.08	1.26	1.45
J O I N T	Hoops	3 layers 6-D10@80			3 layers 4-D10@80	3 layers 6-D10@80	
	Reinf. Ratio pw(%)	0.93			1.12	1.07	0.93
	Shear Capacity Ratio	0.88			0.75	0.82	0.88
	τ_{pbu} / Fc	0.42			0.51	0.46	0.42
Failure Type		Joint Shear Failure					

$\tau_{pbu} = (2M_{bu} - Q_c\, j_b) / t_p\, j_c\, j_b$

$M_{bu} = 0.9\, a_t\, \sigma_y\, d_b$

$Q_{bu} = M_{bu} / l_b$, $Q_c = Q_{bu}\, L / H$

$j_b = 7/8\, d_b$, $j_c = 7/8\, d_c$, tp= joint width

Shear Capacity Ratio $= \tau_u / \tau_{pbu}$

$\tau_u = 95 + 0.5\, p_w\, \sigma_y$ (kgf/cm²)

(Kamimura's Formula)

Fc: Specified Concrete Strength

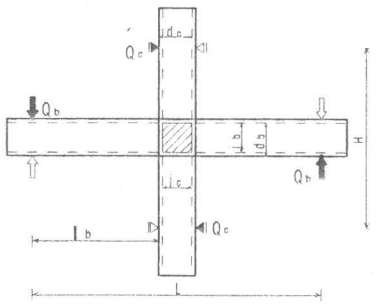

The second group was composed by JPC–34, JPC–35 and JPC–36. JPC–34 had a very thin column with a cross section of 42 cm x 50 cm, without eccentricity. JPC–35 and JPC–36 had the beams shifted in the same direction (one side eccentricity). The eccentricities from the center of the column were 4 cm and 8 cm, respectively.

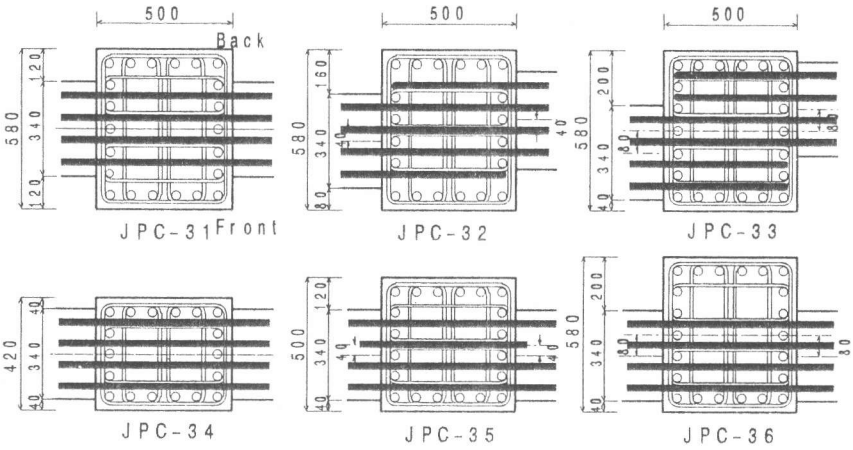

Fig. 3 Section of columns

The sections of beams were identical for all specimens, as shown in Fig. 4. The longitudinal bars were 8–D22 (SD390), placed in two layers, with pt = 2.19%. The lateral reinforcement was 4–D13 (SD295A) spacing every 8–cm. For all specimens, the lateral reinforcement of beam–column joints were 6–D10 (SD295A welded closed hoops) at every 8–cm, placed in 3 layers, except for JPC–34 which had three layers of 4–D10. All precast beams were provided with a shear cotter at the end surface, with 24–cm length, 12–cm height and 8–mm depth.

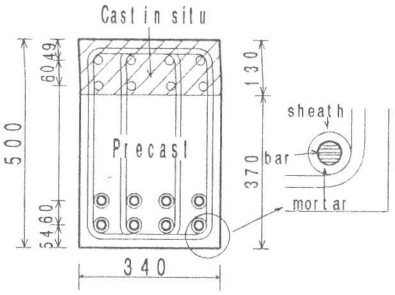

Fig. 4 Section of beams

Table 2 Properties of concrete

Specimen	Precast Exp. day	in Situ Exp. day
JPC–31	440	284
JPC–32	373	300
JPC–33	412	301
JPC–34	431	294
JPC–35	375	287
JPC–36	435	306

Units : kgf/cm^2

Table 3 Properties of steel

Bar Diam	Grade	σ y tf/cm^2	σ b tf/cm^2	E tf/cm^2
D22	SD390	4.45	5.99	1860
D19	SD345	3.72	5.25	1730
D13	SD295A	3.57	–	1760
D10	SD295A	3.76	5.03	1880

σ y : Yield Strength, σ b : Tensile Strength

E: Young's Modulus

The concrete and bar properties are detailed in Tables 2 and 3. The specified compressive strength of concrete and grout mortar were 300 kgf/cm^2 and 600 kgf/cm^2, respectively.

The specimens were subjected to cyclic loads by means of vertical forces at both beam ends. The loading history given is shown in Fig. 5. The lateral drift angle R is defined as the sum of the displacement of beams $\delta 1+\delta 2$ over the distance L between the loading points ($R=(\delta 1+\delta 2)/L$). The axial force applied on the top of the column was $\sigma_0=N/bD=60$ kgf/cm^2 and was maintained constant during the experiment.

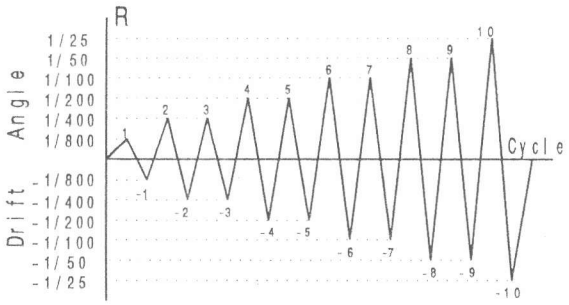

Fig. 5 Loading history

To restrain the movement out of the plane and in the loading plane as well, both ends of the column were supported by oil jacks located at both sides. Clip gauges were placed diagonally to measure the joint shear distortion.

3. TEST RESULTS

3.1 CRACK PATTERN

The crack patterns at the drift angle R=1/50 are shown in Fig. 6. The flexural cracks in the beams appeared in the first stage of loading R=1/800 rad. for all specimens. For JPC–31, JPC–32, JPC–33 and JPC–34 the joint shear cracks started at R=1/400. For JPC–35 and JPC–36 the shear cracks were noticeable at the later stage of the second cycle of R=1/400 and R=1/200, respectively. Because the cracks were delighted on the back side. At R=1/100 the amount of shear cracks became significant. At this point the joint lateral reinforcements started yielding. JPC–31, JPC–32, and JPC–33 presented no cracking in the column. On the other hand, in JPC–34 and the specimens with one side eccentricity (JPC–35, JPC–36) flexural cracks started from R=1/100. For the later two specimens from the cycle of R=1/50 steeper cracks propagated from the joint to the column. These cracks were almost parallel to column reinforcement.

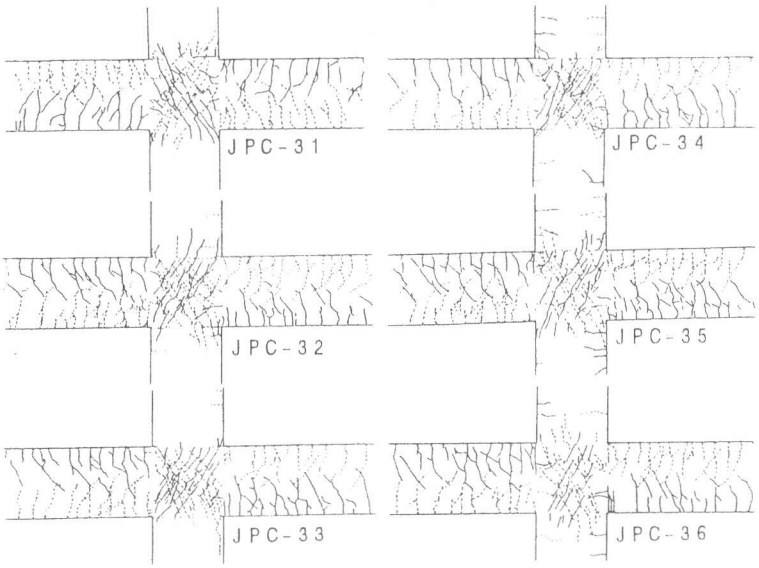

Fig. 6 Crack patterns at R=1/50

3.2 BEAM LOAD – BEAM DISPLACEMENT RELATIONSHIP

Figure 7 shows the beam load–beam displacement relationships. Table 4 shows the experimental and the theoretical values calculated using the flexural ultimate strength theory. No differences can be appreciated for JPC–32 and JPC–33 compared with JPC–31. The beam bars started yielding at R=1/100 before yielding of the joint lateral reinforcement. For these specimens the ratio between the experimental and calculated values of beam flexural strength were very close to each other.

For JPC–34 the joint reinforcement yielded at

Table 4 Beam ultimate strength

Spec.	R	Beam Ultimate Strength Qbu(Tonf)		
		Exp.	Calc.	Exp./Calc.
JPC–31	+1/50	31.34	30.83	1.02
	–1/50	–29.29		0.95
JPC–32	+1/50	31.22	30.53	1.02
	–1/50	–29.22		0.96
JPC–33	+1/25	31.95	30.81	1.04
	–1/50	–29.78		0.97
JPC–34	+1/50	26.48	30.94	0.86
	–1/50	–25.90		0.84
JPC–35	+1/25	30.69	30.55	1.00
	–1/50	–29.28		0.96
JPC–36	+1/25	31.17	30.97	1.01
	–1/50	–28.94		0.93

Qbu=Mbu / lb , Mbu calculated by "e–Function" Method

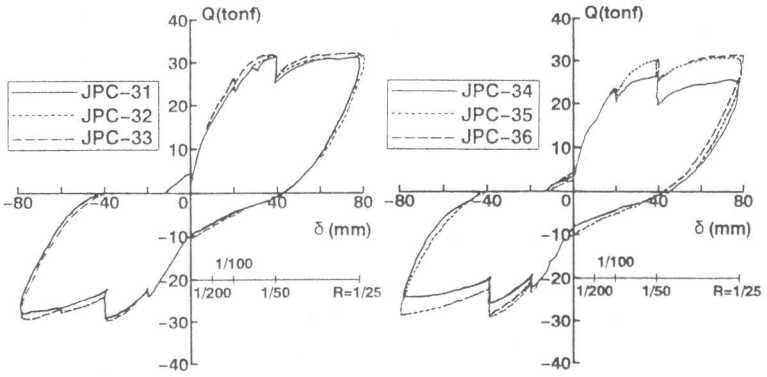

Fig. 7 Beam load–beam deflection relationship

R=1/100, before the beam bars reached the yield point. No strength decay was observed, although the maximum strength was 86 % of the theoretical beam flexural strength. For JPC–35, the joint reinforcement also yielded at R=1/100 before the beam bars, which yielded at R=1/50. On the other hand for JPC–36, the joint reinforcement and the beam bars yielded at R=1/100 almost at same stage.

3.3 BEAM–COLUMN JOINT SHEAR DISTORTION AND SHEAR STRENGTH

The beam load–joint shear distortion relationships are shown in Fig. 8. The shear distortion measured in the front and back sides are presented. JPC–32 and JPC–33 with opposite side eccentricity showed no differences between the front and back sides. JPC–34 at R=1/50 failed in shear and the increase of the shear distortion of the joint became remarkable. Therefore the beams could not develop its full strength. JPC–35 and JPC–36, because of the one side eccentricity, showed more influence of the shear distortion at the front side.

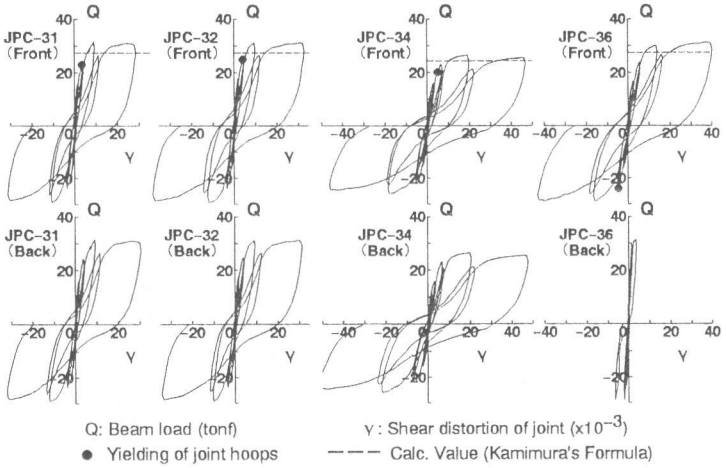

Fig. 8 Beam load–joint shear distortion relationship

Table 5 Joint shear strength

Spec.	Cracking Shear Strength		①		Ultimate Shear Strength		③		④		Failure Mode
	Qb	$_c\tau_c$	$_e\tau_c$	$_e\tau_c / _c\tau_c$	$_e\tau_p$	$_e\tau_p / \sigma_B$	$_c\tau_p$	$_e\tau_p / _c\tau_p$	$_c\tau_p$	$_e\tau_u / _c\tau_p$	
JPC–31	+12.0	48.8	39.9	0.82	131.5	0.45	112.5	1.17	118.4	1.11	B–J
	−10.2		34.0	0.70	122.9	0.42		1.09		1.04	
JPC–32	+ 8.2	49.3	27.4	0.56	131.0	0.44	112.5	1.16	118.0	1.11	B–J
	− 8.2		27.3	0.55	122.6	0.41		1.09		1.04	
JPC–33	+11.4	49.4	38.1	0.77	134.0	0.45	112.5	1.19	120.7	1.11	B–J
	−13.1		43.5	0.88	124.9	0.42		1.11		1.04	
JPC–34	+11.0	49.0	50.8	1.04	134.5	0.46	116.2	1.16	122.2	1.10	J
	−10.2		47.0	0.96	131.5	0.45		1.13		1.08	
JPC–35	+10.0	50.3	38.8	0.77	141.0	0.44	114.2	1.24	126.2	1.12	B–J
	−14.2		46.9	0.93	134.5	0.42		1.18		1.07	
JPC–36	+14.2	50.3	47.4	0.94	130.8	0.41	112.5	1.16	124.9	1.05	B–J
	−14.0		46.6	0.93	121.4	0.38		1.08		0.97	

Qb:Beam Load (tonf), τ:Joint Shear Stress (kgf/cm^2)

$_e\tau_p = (2M_b - Q_c\, j_b) / t_p\, j_c\, j_b$, ① : tp=Column Width

$_c\tau_c = \sqrt{F_t^2 + F_t\,\sigma_0}$, $F_t = 1.6\sqrt{\sigma_B}$

③ : Kamimura's Formula $_c\tau_p = 95 + 0.5 p_w \sigma_y$ ③ & ④ : tp=Effective width

④ : Teraoka's Formula $_c\tau_p = k_p \left(0.115 + \frac{20}{\sigma_B}\right) \frac{d_b + d_c}{\sqrt{j_b^2 + j_c^2}} \sigma_B + 1/4 p_w \sigma_y$

J Type: $k_p = 1.12\, _b p_t^{0.229}$, J&B–J Type $kp = 1.02\, _b p_t^{0.306}\, _c p_t^{0.182}$

J:Joint Shear Failure , B:Beam Flexural Failure

Table 5 Joint shear strength

For a similar input shear, the experimental joint shear stress of JPC–36 becomes smaller than that obtained for JPC–35, because the effective joint width is bigger. Therefore the joint width of specimen JPC–36 seems to be overestimated.

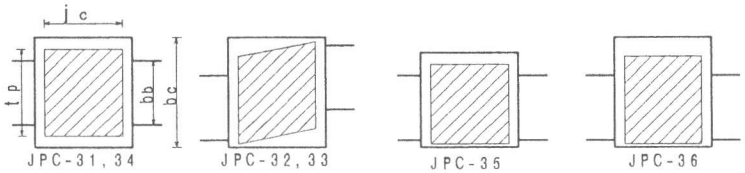

Fig. 9 Effective width of joints

3.4 STRAIN DISTRIBUTION OF JOINT LATERAL REINFORCEMENT

The strain distributions of the hoops in the beam–column joint are shown in Fig. 10. There were three layers of hoops called in this figure as upper, middle and lower layers. The strain distributions correspond to the direction of loading and the letters A to E corresponds to the position of each leg of the lateral reinforcement. In both cases of eccentricity, all the legs were effective to resist the beam–column joint shear stress. Figure 11 shows the strain distribution of the legs, perpendicular to the direction of loading. It is observed that strains at all the legs in perpendicular direction are a little smaller than those in the loading direction, but effective to resist the shear stress by confining the beam–column joint.

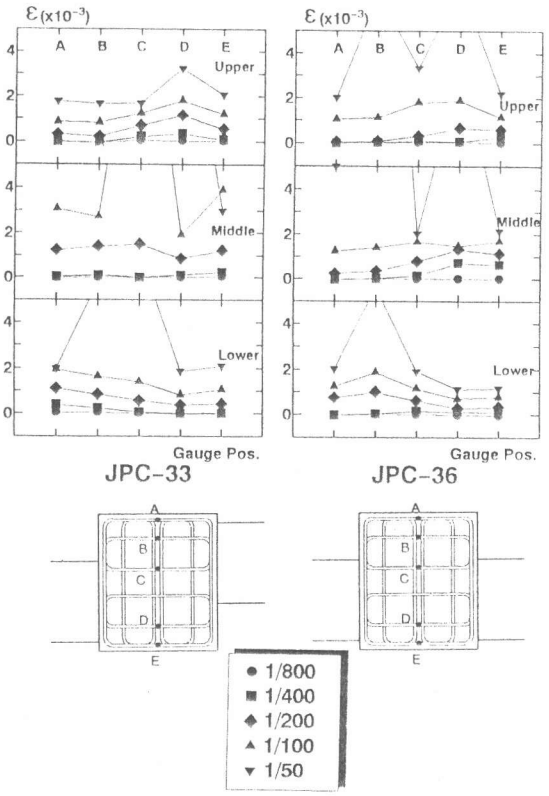

Fig. 10 Strain distribution of joint hoops

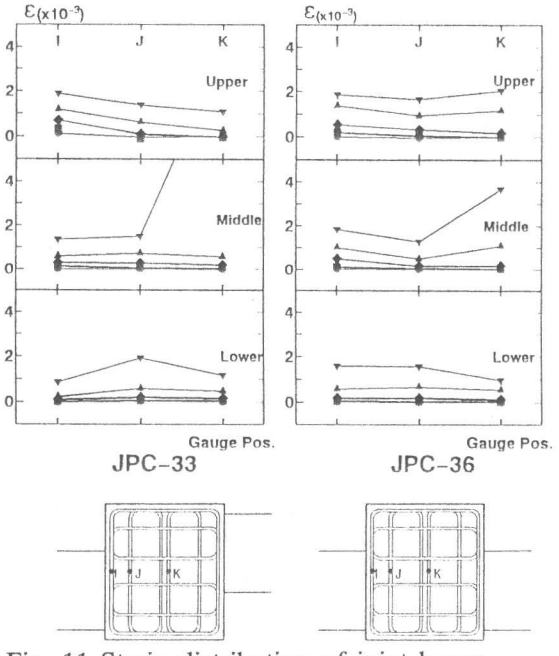

Fig. 11 Strain distribution of joint hoops

4. CONCLUSIONS

From the test results the following conclusions can be drawn:

1) For the grade of eccentricity given to the specimens, the hysteretic curves showed no influence in the case of opposite side eccentricity.
2) For specimens with one side eccentricity, there was no further influence of the eccentricity, however as much as the column section was increased the average width value produced an overestimation of the effective joint width.
3) Independent of the eccentricity all the legs of the hoops of beam–column joints in both, the loading and the perpendicular, directions proved to be effective to resist the joint shear stress.

REFERENCES

1) Castro J.J., Yamaguchi T., Imai H.,"Seismic Performance of Precast Concrete Beam–Column Joints", Trans. of AIJ, No. 455, Jan.,1994, pp. 113–126.
2) Ozawa T., et al. ," Behaviors of Reinforced Concrete Column–Beam Joints with Various Details under Cyclic Loads", (in Japanese), Proc. of AIJ, Sep. 1983, pp.1809–1812.
3) Kamimura, H, "Ultimate Shear Strength of Beam–Column Joints for Monolithic Reinforced Concrete Structures", (in Japanese), Proc. of AIJ, Oct. 1975, pp.1155–1156.
4) Teraoka M. et al., "Study on Mechanical Properties of Reinforced Concrete Cross Type Beam–Column Joints", Proc. of AIJ, Aug. 1986, pp.115–120.